

# Variable Angle of SRG for Wind Energy Control Application

Maged N. F. Nashed  
Electronics Research Institute, Cairo, Egypt  
maged@eri.sci.eg

**Abstract**— *Switched reluctance machine has various desirable features, which comes from its simple construction. They are the wide speed range, high temperature operation and small moment of inertia. There are many control variables, such as: firing angles, reference current, speed and voltage. This paper presents a nonlinear model of 6/4 Switched Reluctance Generator (SRG) with two converter (one with generator side and other with grid side) based on wind Energy system. This system provides a new approach to maximize the amount of power generated. Closed loop control with based PI current Control model is used. A Power converter in SRG can be produced maximum power efficiency and minimize the ripple contents in the output of SRG depend on the converter angles. A second power converter namely PI based controlled PWM inverter is used to interface the machine to the Grid. This system proposed feasibility and validity are simulated on MATLAB/SIMULINK.*

**Keywords**—Wind Energy, SRG, SHB, and VSC.

## I. Introduction

Wind energy is one of the renewable energy must used actually. The electrical induction machines and synchronous generators are widely used in wind turbines. Wind generators have been widely used both in autonomous systems for power supplying remote loads and in grid-connected applications. Wind generator systems are Induction Generators (IG), Double Fed Induction Generators (DFIG) or Permanent Magnet Synchronous Generators (PMSG). The speed of IG is close to fixed value of speed. Thus, the wind power utilization factor cannot be maintained at the optimal value during wind speed variation. The DFIG can change its operating speed and has better utilization factor of wind energy. However, the structure of DFIG is complex and a gear box is required which results in reducing system reliability and more maintenance works. The variable speed of PMSG can be directly driven without gearbox, but its material cost is high and more efforts are required to improve its performance, reliability and reduce its cost and size.

SRG has been studied and pointed as a good solution for applications of wind generation systems up to 500kW, [1]. SRG has as main characteristics: mechanical robustness, high starting torque, high performance and high power density [2-4]. These features make it very suitable for the application of direct-driven wind turbines. SRG can operate at variable speeds and its operating range is broader than synchronous and induction generators. Some works that study the behavior of the SRG in case of variable speed were presented in [5-7]. The analyze SRG operating performance of are presented.

In this work is performed a control method of SRG through simulation techniques using mathematical models of the studied system. A wind power generation with SRG connected to the grid

was performed based on control of two separate converters. The control of the converter connected to SRG regulates the extraction of electrical power to be generated and the control of the converter connected to the grid is responsible for regulate the transmission of the generated energy to the grid.

Fig. 1, shows 6/4 SRG. The winding A-A' in Fig. 1 is one of the machine phases. Fig. 2 shows the idealized inductance profile of a SRG. If saturation is neglected then the inductance varies linearly with respect to the overlap between the stator and rotor poles. The inductance is maximum when the rotor and stator poles are fully aligned and minimum when the poles are completely unaligned. For generation, the machine phases are excited during the negative slope of the inductance profile, [2]. Fig. 3 shows the block diagram of the system. It is consist of wind turbine, SRG, asymmetric H-Bridge (AHB), and PWM inverter with control system

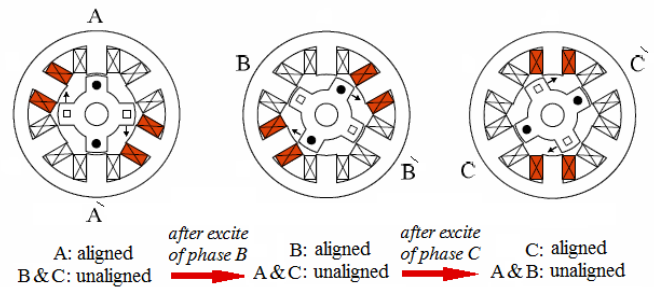


Fig. 1. The 6/4 SRG.

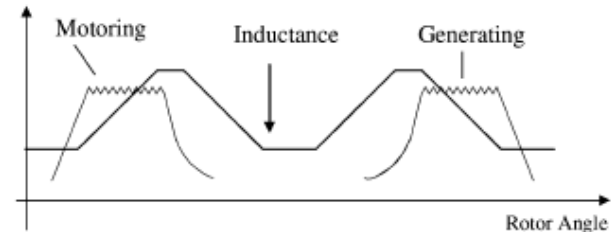


Fig. 2. Illustrative shape and position of current waveforms with respect to inductance profiles for SRG operation.

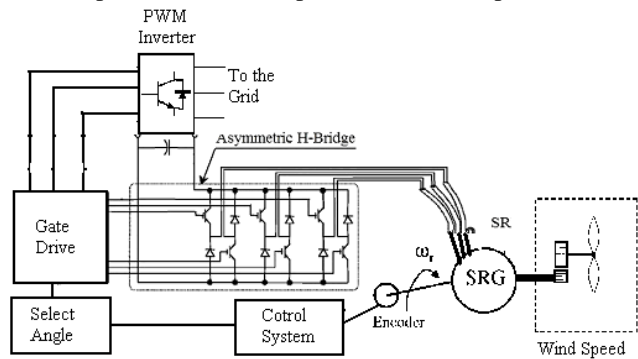


Fig. 3, Block diagram of the system.

## II. System Construction

### 1. Wind Turbine Power

To use the energy contained in wind is necessary to have a continuous and fairly strong wind flux. The modern wind turbines are designed to achieve the maximum power in wind speeds in the order of 10 to 12 m/s. The mathematical model allows calculating the aerodynamic torque mechanical value or mechanical power applied to the shaft of the electric generator from the information of the wind speed and position value of the step angle of the turbines. The model also depends on the type of the turbine to be represented as having the characteristics of vertical or horizontal axis, number of blades, blade angle control, and regardless of the type of electrical generator chosen or the type of control of converters. Accordingly, this allows it to be studied regardless of the types of electrical generators. The mechanical power in steady state can be extracted from the wind is, [8]:

$$P_m = \frac{1}{2} \rho A v^3 C_p(\lambda, \beta) \quad (1)$$

Where,  $P_m$  mechanical power of the turbine,  $\rho$  density of air,  $A$  area swept by the turbine blades,  $v$  wind speed and  $C_p$  coefficient of performance,  $\lambda$  a tip speed ratio, and  $\beta$  blade pitch angle. The power coefficient of  $C_p$  indicates the efficiency with which the wind turbine transforms the kinetic energy contained in wind into mechanical energy rotating. Therefore, for wind speeds below rated speed operation with variable speed rotor increases efficiency in power generation [8]. The profile of optimizing the efficiency of the power generated for variable speeds can be expressed by:

$$P_{opt} = k_{opt} \omega^3 \quad (2)$$

Where  $P_{opt}$  is the optimum power and  $k_{opt}$  depends of aerodynamics of the helix, gearbox and parameters of the wind turbine. The power curve speeds of a typical wind turbine are shown in Fig. 4. The value of maximum wind turbine output power per unit can be obtained by putting zero pitch angle and Betz limit, when the velocity of wind turbine is 12 m/s. The mechanical output power  $P_m$  of the wind turbine, which is the input power to the generator, varies with wind speed as shown in Fig 4.

### 2. Characteristics of Generating Operation

For the SRG in table 1, [9], the work done and the torque can be evaluated from the area enclosed between the aligned and unaligned flux linkages versus excitation current characteristics as shown in Fig. 5.

In a SRG, The electrical equation for a phase of the 6/4 SRG is, [10]:

$$v_a = R_a i_a + \frac{d\theta}{dt} (L_{aa} \frac{di_a}{d\theta} + L_{ab} \frac{di_b}{d\theta} + L_{ac} \frac{di_c}{d\theta}) + \frac{d\theta}{dt} (\frac{dL_{aa}}{d\theta} i_a + \frac{dL_{ab}}{d\theta} i_b + \frac{dL_{ac}}{d\theta} i_c) \quad (3)$$

where  $v_a$  is the phase  $a$  winding voltage;  $i_a$ ,  $i_b$ , and  $i_c$  are the phases currents;  $R_a$  is the resistance of the winding;  $L_{aa}$  is the self inductance of phase  $a$ ;  $L_{ab}$  is the mutual inductances among phases  $a$  and  $b$ ;  $L_{ac}$  is the mutual inductances among phases  $a$  and  $c$ ;  $\theta$  is the rotor angular position and the so the rotor angular speed is:

$$\omega = \frac{d\theta}{dt} \quad (4)$$

The induced electromotive force is given by:

$$e = \frac{d\theta}{dt} (\frac{dL_{aa}}{d\theta} i_a + \frac{dL_{ab}}{d\theta} i_b + \frac{dL_{ac}}{d\theta} i_c) \quad (5)$$

The stator winding is fed in DC. When the back electromotive force is negative it increases the current converting mechanical power into electrical power and the machine acts as a generator. The dynamic mechanical equation for the SRG is to be noted that the electromagnetic torque  $T_e$  comes as a negative quantity, so acting against the rotor mechanical speed.

$$T_m = T_e + J \frac{d\omega}{dt} + D\omega \quad (6)$$

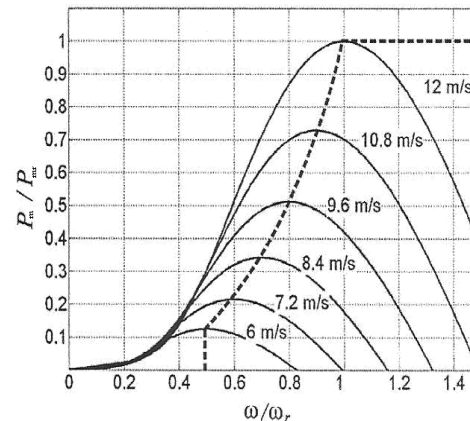


Fig. 4, Output Power vs. turbine speed at different wind speeds

Table 1, The parameters of the three phase 6/4 poles SRG

Number of motor phases	3
Number of stator poles $N_s$	6
Number of rotor poles $N_R$	4
Stator phase resistance	$17 \Omega$
Aligned inductance	$0.605 H$
Unaligned inductance	$0.155 H$
Inertia constant	$J = 0.0013 \text{ Kg.m}^2$
Viscous friction coefficient	$0.0183 \text{ N.m.Sec}^2$
Rated phase current	3 A

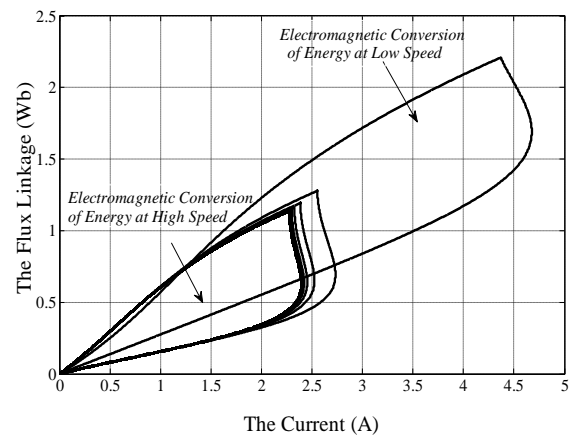


Fig. 5, Evolution of energy conversion at different speeds.

where  $T_m$  and  $T_e$  are the mechanical torque and the electromagnetic torque respectively,  $J$  is the inertia and  $D$  is the coefficient of friction. And the corresponding electromagnetic torque for a three phase SRG is given by:

$$T_e = \sum_{x=1}^3 \frac{dW_x^{co}}{d\theta} \quad (7)$$

where  $W^{co}$  is the co-energy of a phase of SRG.

The mathematical model of the SRG regarding a three phase prototype is shown below:

$$\begin{bmatrix} v_a \\ v_b \\ v_c \\ T_m \\ 0 \end{bmatrix} = \begin{bmatrix} R_a & \omega \frac{dL_{ab}}{d\theta} & \omega \frac{dL_{ac}}{d\theta} & 0 & 0 \\ \omega \frac{dL_{ba}}{d\theta} & R_b & \omega \frac{dL_{bc}}{d\theta} & 0 & 0 \\ \omega \frac{dL_{ca}}{d\theta} & \omega \frac{dL_{cb}}{d\theta} & R_c & 0 & 0 \\ \frac{dW_a^{co}}{d\theta} & \frac{dW_b^{co}}{d\theta} & \frac{dW_c^{co}}{d\theta} & D & 0 \\ 0 & 0 & 0 & -1 & 0 \end{bmatrix} + \begin{bmatrix} i_a \\ i_b \\ i_c \\ \omega \\ \theta \end{bmatrix} \quad (8)$$

$$\begin{bmatrix} L_{aa} & L_{ab} & L_{ac} & 0 & i_a \frac{dL_{aa}}{d\theta} \\ L_{ba} & L_{bb} & L_{bc} & 0 & i_b \frac{dL_{bb}}{d\theta} \\ L_{ca} & L_{cb} & L_{cc} & 0 & i_c \frac{dL_{cc}}{d\theta} \\ 0 & 0 & 0 & J & 0 \\ 0 & 0 & 0 & 0 & 1 \end{bmatrix} \begin{bmatrix} i_a \\ i_b \\ i_c \\ \omega \\ \theta \end{bmatrix}$$

### 3. Power converters

The converter used to drive SRG was the AHB converter. This converter is connected via the DC link with the voltage source converter that it is connected to the grid. This system is shown in Fig. 6. The diagram of the direct power control is shown in Fig. 7. The control consists in table select the value of angle  $\theta_{on}$  and  $\theta_{off}$  depend on the wind speed, [11]. These values are in table 2.

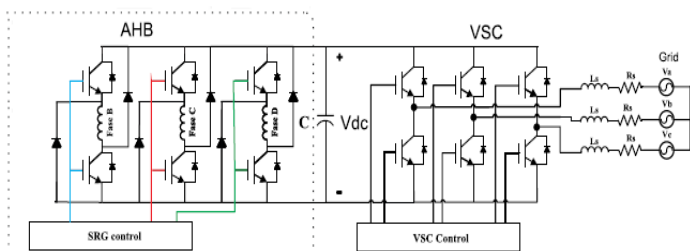


Fig. 6, Power converters.

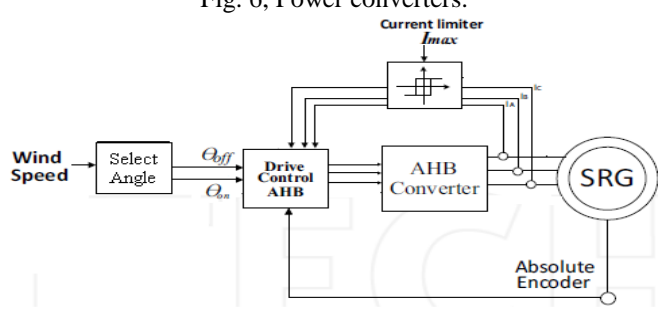


Fig. 7, Diagram of direct power control for SRG.

Table 2, The select of  $\theta_{on}$  and  $\theta_{off}$  at different speed (rad/sec).

$\theta_{off}$ $\theta_{on}$	60°	64°	68°	72°	74°	78°	82°
16°	83	87	91	95	97	100	102
20°	77	81	85	89	91	94	96
24°	70	75	78	82	85	88	91
28°	64	68	73	76	79	82	85
32°	57	62	66	70	74	76	78
36°	51	55	60	64	67	70	73
40°	44	49	53	57	61	64	68
44°	37	42	47	51	55	58	61
48°	31	36	40	45	48	52	55
52°	25	29	34	38	42	46	49
56°	17	22	27	32	36	40	43

The power grid Converter, shown in Fig. 8, controls the voltage  $V_{dc}$  and it allows sending the generated power by SRG to the grid. The control strategy applied to the converter voltage source consists of two control loops. The current loop control ( $i_{sd}$ ,  $i_{sq}$ ) is responsible for controlling the power factor of the power sent to the grid. The control voltage of the DC link is responsible for balancing the flow of power between the SRG and the grid, [12]. The control voltage of the DC link is performed by a PI controller, which comes from the reference value  $i_{sd}^*$ , while the value of  $i_{sq}^*$  is derived from the power factor desired and  $P_{ref}$ .

$$i_{sq}^* = \frac{-3}{2} P_{ref} \frac{\sqrt{1-PF^2}}{PF^2} \quad (9)$$

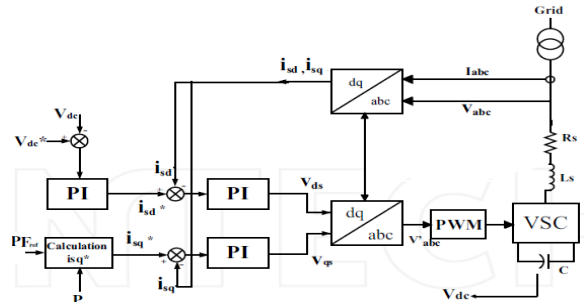


Fig. 8, Block diagram of vector control of power grid converter.

### III. System Results:

The power control system proposed for the SRG connected to the grid was simulated using Matlab/Simulink software. The output power by the SRG and reference power with variable wind speed are shown in Fig. 9. While, Fig. 10 is shown the rotor speed of SRG depend on change of wind speed. The time of steady state is take less than 0.1 sec. Figure 11 shows the inverter phase currents of AHB, it which observe the variation of current amplitudes, a fact that is justified due to the fact the controller changes in the value of angle  $\theta_{on}$  and  $\theta_{off}$ . The torque of SRG is shown in Fig. 12. While, the output voltage of DC link is shown in Fig. 13. The DC link value is  $L = 5$  mH and  $c = 5000 \mu F$ . Fig. 14 is shown the output voltage of VSC and with filter. The Total Harmonic Distortion of the voltage is shown in Fig. 15. The value of harmonic is 2.83%.

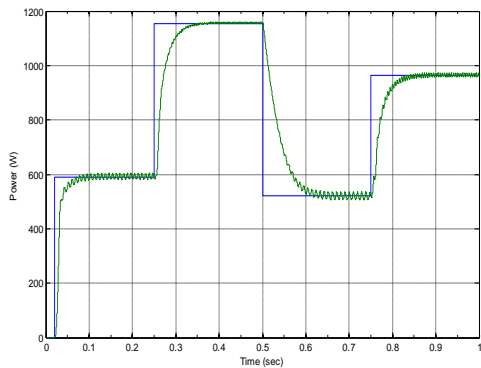


Fig. 9, Power generated and reference power.

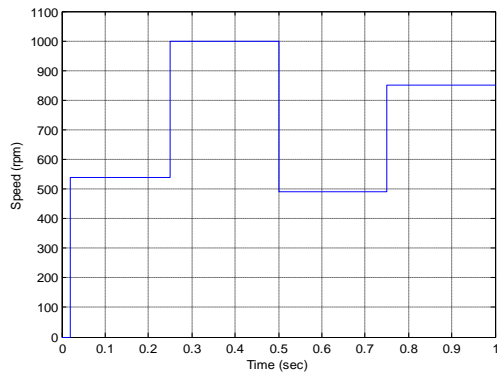
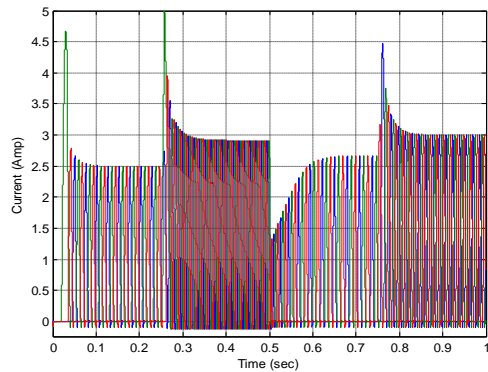
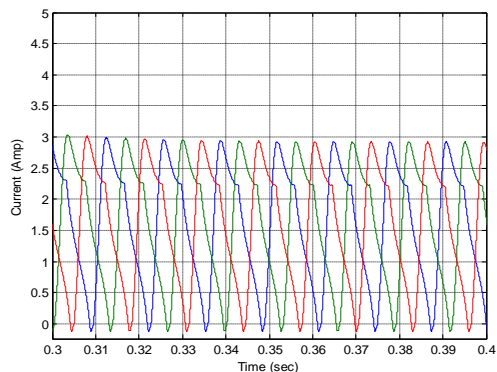


Fig. 10, The rotor speed of SRG.



(a)



(b)

Fig. 11, The inverter phase currents of AHB with zoom in (b).

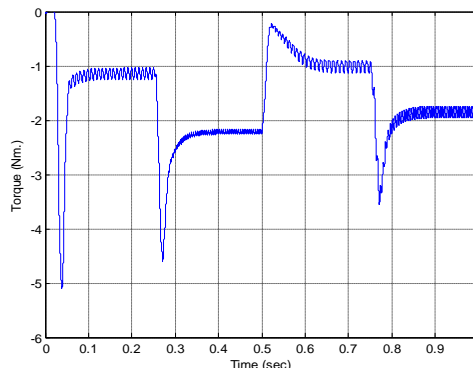


Fig. 12, Torque of SRG.

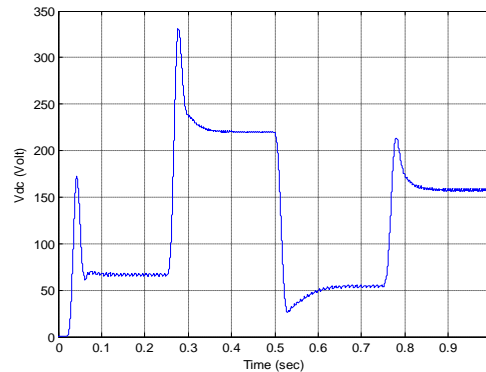
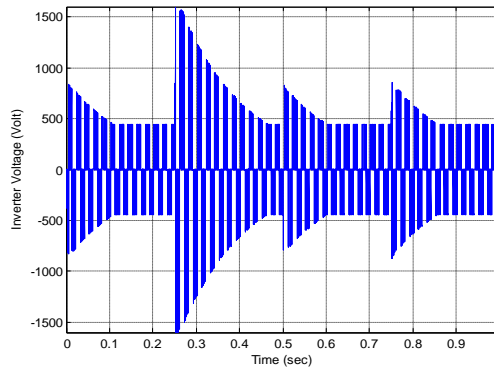
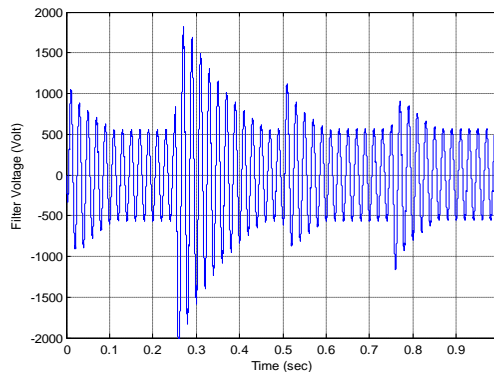


Fig. 13, Output voltage of DC link.



(a) PWM inverter



(b) after filter.

Fig. 14, The output voltage of VSC.

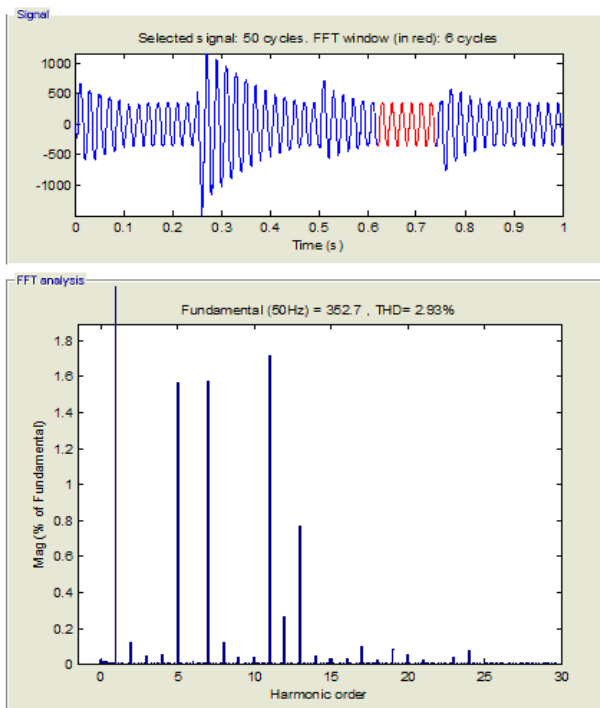


Fig. 15, Harmonic components of VSC voltage.

#### IV. Conclusions

This paper was presented a proposal for direct control of power for a SRG based wind turbine system for output power. The power control of the generator is directly without using current loops. A model of SRG has built using MATLAB/SIMULINK Software. The controller has a satisfactory performance and no complexity. The Generator performance, including output power, was simulated in terms of turn on and turns off angles for different wind speeds. The AHB converter was robustness, the stages of regeneration energy and freewheels when needed. The simulation results confirm the effectiveness of the power controller during conditions of generator operation at variable wind speed. Thus, the strategy of direct control of power is an interesting tool to control the power of the variable reluctance generator powered wind turbines.

#### References

- i. Association World Wind Energy. "The World Wind Energy 2011" report, 2012.
- ii. A. Arifin, I. Al-Bahadly, and S. C. Mukhopadhyay, "State of the Art of Switched Reluctance Generator" *Energy and Power Engineering, Scientific Research*, Vol. 4, Nov. 2012, pp: 447-458.
- iii. E Echenique, J. Dixon, R. Cárdenas, and R. Peña, "Sensorless Control for a Switched Reluctance Wind Generator, Based on Current Slopes and Neural Networks" *IEEE Transactions on Industrial Electronics*, Vol. 56, No. 3, Mar. 2009, pp: 817-825.
- iv. D.A Torrey, "Switched Reluctance Generators and their Control," *IEEE Transactions on Industrial Electronics*, Vol. 49, 2002 pp: 3-14.
- v. K. Kaliyappan and S. Padmanabhan, "PI-CCC Based Switched Reluctance Generator Applications for Wind Power Generation Using MATLAB/SIMULINK" *Journal Electrical Engineering Technology*, Vol. 8, No. 2: 2013, pp .230-237.
- vi. K. Ogawa, N. Yamamura, and M. Ishida. Study for small size wind power generating system using switched reluctance generator. *IEEE International Conference on Industrial Technology*, 2006, pp: 1510–1515.
- vii. R. Cardenas, R. Pena, M. Perez, G. Claro, J. Asher, and P. Wheeler. Control of a switched reluctance generator for variable-speed wind energy applications. *IEEE Transactions on energy conversion*, Vol. 20, No. 4, Dec. 2005, pp: 691 –703.
- viii. Manfred Stiebler. "Wind Energy Systems for Electric Power Generation", Springer, 2008.
- ix. Maged N. F. Nashed, Samia M. Mahmoud, Mohsen Z. El-Sherif, and Emad S. Abdel-Aliem, "Optimum Change of Switching Angles on Switched Reluctance Motor Performance" *International Journal of Current Engineering and Technology (IJCET)*, Vol.4, No.2, April 2014, pp: 1052-1057.
- x. A. Fleury, D. A. Andrade, A. W. F. V. Silveira, P. H. F. Ribeiro, F. S. L. F. Melo, L. A. G. Migliorini, D. N. Dias, and J. I. Oliveira, "Wind Powered Switched Reluctance Generator for Rural Properties and Small Communities" *International Conference on Renewable Energies and Power Quality (ICREPQ'10)*, Spain, 23-25 March, 2010.
- xi. A. Arifin, I. H. Al-Bahadly, and S. C. Mukhopadhyay "Simulation of Switched Reluctance Generator in Low and Medium Speed Operations for Wind Energy Application" *International Scholarly Research Network, ISRN*, Vol. 2012, Article ID 327296.
- xii. M. L. Adrian, V. T. F. Blaabjerg, and R. Teodorescu, "Overview of control and grid synchronization for distributed power generation systems", *IEEE Transactions on industrial electronics*, Vol. 53, No. 5, Oct. 2008, pp: 691 –703.